HHS Public Access

Author manuscript

Ann Thorac Surg. Author manuscript; available in PMC 2020 January 01.

Published in final edited form as:

Ann Thorac Surg. 2019 January ; 107(1): 224–232. doi:10.1016/j.athoracsur.2018.06.015.

A Clinical Trial of TumorGlow® to Identify Residual Disease during Pleurectomy and Decortication

Jarrod D. Predina, MD, MTR[1,2], **Andrew D. Newton, MD**[1,2], **Christopher Corbett, BA**[1,2], **Leilei Xia, MBBS**[1,2], **Michael Shin, BA**[1,2], **Lydia Frenzel Sulfyok, BA**[1,2], **Olugbenga T. Okusanya, MD**[3], **Keith A. Cengel, MD, PhD**[4], **Andrew Haas, MD**[5], **Leslie Litzky, MD**[6], **John C. Kucharczuk, MD**[1,2], and **Sunil Singhal, MD**[1,2,*]

[1]Center for Precision Surgery, Perelman School of Medicine at the University of Pennsylvania (Penn)

[2]Department of Surgery, University of Pennsylvania

[3]Department of Surgery, University of Pittsburgh Medical Center

[4]Department of Radiation Oncology, University of Pennsylvania

[5]Division of Pulmonology, Allergy, and Critical Care, University of Pennsylvania

[6]Division of Pathology and Laboratory Medicine, University of Pennsylvania

Abstract

Background—Macroscopic complete resection can provide a select group of malignant pleural mesothelioma (MPM) patients improved survival. During resection, differentiating residual tumor from inflammation or scar can be challenging. In this trial we evaluate near-infrared (NIR) intraoperative imaging using TumorGlow® technology to improve detection of macroscopic residual disease.

Methods—Twenty subjects were enrolled in an open-label clinical trial of NIR intraoperative imaging with TumorGlow® imaging (NCT02280954). Twenty-four hours prior to pleural biopsy or pleurectomy and decortication (P/D), patients received intravenous indocyanine-green (ICG). All specimens identified during standard-of-care surgery and with NIR imaging underwent histopathologic profiling and correlative microscopic fluorescent tomographic evaluation. For subjects undergoing P/D (n=13), the hemithorax was evaluated with NIR imaging during P/D to assess for residual disease. When possible, additional fluorescent lesions were resected.

Results—Of 203 resected specimens submitted for evaluation, ICG accumulated within 113 of 113 of resected mesothelioma specimens, with a mean signal-to-background fluorescence ratio (SBR) of 3.1 (SD, 2.2–4.8). The mean SBR of benign tissues was 2.2 (SD, 1.4–2.4), which was significantly lower than within malignant specimens (p=0.001). NIR imaging identified occult

*Corresponding Author: Sunil Singhal, MD, 6 White building; 3400 Spruce St. Philadelphia, PA 19104. sunil.singhal@uphs.upenn.edu.

macroscopic residual disease in 10 of 13 subjects. A median of 5.6 resectable residual deposits per patient (range, 0–11 deposits/patient) with mean size of 0.3cm (range 0.1–1.5cm) were identified.

Conclusions—TumorGlow® for MPM is safe and feasible. Excellent sensitivity allows for to reliable detection of macroscopic residual disease during cytoreductive surgery.

Keywords

mesothelioma; surgery; intraoperative imaging; optical imaging; ICG

Classifications

Cancer; Imaging; Mesothelioma; Surgery/incisions/exposure/techniques

Malignant pleural mesothelioma (MPM) is a rare disease that is associated with a dismal 5-year-survival rate of 15% (1). Current standard-of-care, consisting of palliative chemotherapy, results in median survivals less than 1 year (2, 3). In select patients with limited disease, multi-modal treatment protocols incorporating chemotherapy, radiation and cytoreduction via pleurectomy and decortication (P/D) or extrapleural pneumonectomy (EPP) have been associated with improved median survivals (2, 4). The overall goal of surgical resection is tumor cytoreduction, or complete macroscopic (R1) resection, which confers a survival advantage. Despite this aggressive approach, most patients still develop local disease recurrence (5, 6). In efforts to improve upon poor outcomes, a number of modifications to this treatment paradigm have been proposed; for example, neoadjuvant hemithoracic radiation (7), hyperthermic intraoperative chemotherapy (8), and post-resection photodynamic therapy (9).

Fluorescence guided surgery (FGS) is an alternative approach which may improve outcomes after cytoreduction by highlighting residual disease that is directly responsible for local disease relapse. FGS involves systemic infusion of optical contrast agents which accumulate in cancerous tissues, thus allowing for real-time identification using optimized lighting and camera systems. Recently, our group has utilized FGS for localization of several common thoracic solid tumor types including pulmonary metastases (10) and non-small cell lung cancer (NSCLC) (11). Our approach, TumorGlow®, involves systemic delivery of the near-infrared (NIR) contrast agent, indocyanine green (ICG), with FGS occurring 24 hours after drug delivery. This approach has demonstrated the capacity to identify occult cancer deposits as small as 2mm. ICG is an appealing optical contrast agent given its excellent safety profile and its propensity to accumulate in a diverse array of tumor histologies via the enhanced permeability and retention effect (EPR) (10, 11). The EPR permits nanostructures to accumulate in most malignancies, as a result of leaky vasculature and the lack of lymphatics (12). In pre-clinical studies, we have demonstrated feasibility in small animal models of MPM (13), however, this approach has not be evaluated in humans.

In this report, we describe our initial experiences involving TumorGlow® in 20 subjects who presented for suspicious pleural based diseases (Cohort 1) and histologically confirmed MPM (Cohort 2). More specifically, we sought to (1) evaluate safety and feasibility of NIR

imaging with ICG in patients with MPM, and (2) determine if ICG accumulates in MPM and allows for reliable detection of residual disease following P/D.

Material and Methods

Study Drug and Imaging Device

Approximately 24 hours prior to surgery, subjects were infused with ICG (5 mg/kg) (Akorn Pharmaceuticals, Illinois) as previously described by our group (14, 15). ICG has an excitation and emission wavelength of 805nm and 830nm, respectively. NIR imaging was performed using the Iridium system optimized for detection of ICG (Visionsense Corp, Philadelphia, PA) as previously described by our (14, 15). The Iridium is a high definition, dual band (white light and NIR) camera system which uses an excitation laser (805nm) and detects fluorescence using a bandpass filter (825 to 850nm). For intrathoracic imaging, the Iridium was equipped with a 5mm, 0-degree thoracoscope. For *ex vivo* evaluation, an exoscope was suspended 20 inches above the patient and was utilized for NIR imaging.

Study Design

This non-randomized, open-label, single-arm, single-center feasibility study (NCT02651246) was approved by the University of Pennsylvania Institutional Review Board. Twenty subjects provided informed consent and were enrolled in two cohorts between January 2016 and April 2017. The primary goals were to establish safety and feasibility of TumorGlow® for pleural based neoplasms and MPM. We were secondarily interested to determine if ICG accumulation allowed for reliable detection of residual disease during P/D.

Safety was assessed by periodic subject evaluation from infusion to postoperative follow-up (2–4 weeks following resection). Adverse events were described using Common Terminology Criteria for Adverse Events (CTCAE), Version 4.03 (16). Feasibility was evaluated across two cohorts: Cohort 1 was recruited to determine if ICG reliably accumulates in MPM and Cohort 2 was recruited to determine if NIR intraoperative imaging with ICG improves MPM surgery by identifying residual disease. Two attending thoracic surgeons, SS and JCK, performed all procedures (9 years and 18 years since board certification, respectively).

In Cohort 1, 7 subjects were recruited. Each subject was referred to our clinic for evaluation of a recurrent pleural effusion with negative cytology. Preoperative imaging demonstrated pleural thickening, and patient history was concerning for MPM. During thoracoscopic biopsy, surgeons first utilized standard white-light visualization to identify lesions of interest. Next, NIR intraoperative imaging was used to determine if identified lesions displayed fluorescence. At least 3 pleural biopsies were included for each subject, with at least one displaying fluorescence and one being non-fluorescent when possible. Test characteristics of NIR optical imaging were calculated using final pathology as a “gold standard”.

In Cohort 2, 13 surgical candidates (Stage I or Stage II MPM as determined by NCCN guidelines (17)) with histologically confirmed epithelioid MPM were enrolled. Subjects

were also deemed resectable after completion of a metastatic work-up. During P/D with lymph node sampling, surgeons initially proceeded with standard-of-care resection. Next, after what was believed to be R1 resection, the thorax was re-evaluated using NIR imaging to assess for residual resectable disease. Suspicious areas identified by fluorescent imaging were resected. All resected specimens were reviewed by a certified thoracic pathologist.

Fluorescent Microscopy

For specimens from enrolled in Cohort 2, 5μm slides from formalin-fixed paraffin embedded (FFPE) blocks of each specimen were requested and analyzed for ICG accumulation using a NIR-capable microscopic scanner (Odyssey CLx, LI-COR). After quantification of fluorescence, slides were stained by H&E to allow for histologic correlation.

Statistical Analysis

Posthoc image analysis was performed to quantify the amount of fluorescence using region of interest (ROI) feature within ImageJ image analysis software (http://rsb.info.nih.gov/ij). A signal-to-background fluorescence ratio (SBR) was calculated, with an SBR of >2.0 considered fluorescent. Data are presented as median (IQR) for samples less than 40 and mean (SD) for larger sample sizes. Sensitivity, specificity, positive predictive value (PPV), and negative predictive value (NPV) for NIR intraoperative imaging were calculated and compared pathologic evaluation (gold-standard). Differences between two groups were compared by the Mann-Whitney test or student's t-test as appropriate. Comparisons were made use Stata: Release 14 (College Station, TX). A p-value of 0.05 was considered statistically significant.

Results

Patients and Safety Data

Twenty subjects (n=14 male), median age of 67.5 years (IQR, 62.5 and 72.5 years), were enrolled. In Cohort 1, pleural biopsies reveal epithelioid MPM (n=3), sarcomatoid MPM (n=2), mixed MPM (n=1), and benign mesothelial inflammation (n=1). In Cohort 2, 13 subjects with MPM underwent P/D for preoperatively identified epithelioid MPM. Each subject in Cohort 2 received preoperative chemotherapy.

Systemic ICG was well tolerated. Only Subject 7 encountered drug toxicity, which was a Grade I Adverse Event involving pain at the injection site during ICG infusion. There was no associated induration, blistering or erythema. Although symptoms improved upon decreasing the infusion rate, the infusion was ultimately aborted given symptom persistence. The patient had the sensation of coldness at the site. In total, 204mg of the ordered 431mg (47.3%) was infused. The pain resolved after infusion cessation and no physical examination or biochemical abnormalities were noted. The procedure was performed as planned, and the patient had no intraoperative or postoperative drug-related toxicity. No other adverse events were encountered.

Table 1 provides a complete summary of subject, pathologic and drug delivery data.

FGS with systemic ICG during pleural biopsy (Cohort 1)

Among the 7 subjects included in Cohort 1, fluorescent lesions could be detected clearly in six subjects (Figure 1a–c). These 6 subjects were found to have MPM upon final histopathologic review of pleural biopsies; 3 subjects with epithelioid histologies, 2 with sarcomatoid histologies, and one with a mixed histology. The single subject (Subject 5) with absent fluorescence signal was found to have only benign mesothelial inflammation (Figure 1d–e).

In total, 40 pleural biopsies were obtained with a median of 5 (range, 4 to 10) biopsies per subject (Figure 1g). The median biopsy size was 0.8cm (IQR, 0.3cm to 1.3cm). Of the 40 pleural biopsies obtained, 29 biopsies displayed fluorescence (defined as an SBR of greater than 2.0); while 11 biopsies displayed no fluorescence. We appreciated fluorescence in lesions as small as 1.5mm (noted in Figure 1a).

Upon final histopathologic review of the 29 fluorescent biopsies, 22 were MPM while 7 were benign. All non-fluorescent biopsies were non-cancer by pathology. Based on this data, the sensitivity of optical imaging for malignancy was determined to be 100% with the NPV also equaling 100%. A PPV of lesion fluorescence was 75.6%, and specificity was 61.1% (test characteristics with 95% CI are summarized in Table 2). Although we appreciated a false-positive rate of 24.1%, we observed no false-negatives. Finally, we determined that the mean SBR of MPM confirmed biopsies was 3.0 versus 1.8 in benign biopsies ($p<0.01$) (Figure 1f).

These data suggested that FGS with ICG is 100% sensitive for MPM, and can reproducibly detect lesions in the sub-centimeter ranger. This information suggested that this approach may provide a tool to that could help identify MPM during cytoreduction and potentially detect residual disease following cytoreduction.

FGS with systemic ICG identifies resected MPM during cytoreductive surgery (Cohort 2)

Before exploring the ability to FGS with ICG to detect residual disease, we sought to confirm that ICG accumulate in MPM during P/D. During cytoreductive surgery, tumor deposits displayed high levels of fluorescence in 13 (100%) subjects upon real-time *in situ* and *ex vivo* analysis (Figure 2a–c). A total of 107 samples (82 fluorescent lesions and 25 non-fluorescent areas) were isolated and submitted for review by a pathologist (Figure 2d–i). Of the 82 fluorescent lesions, 59 (71.9%) were confirmed to MPM with 23 (28.0%) found to be benign inflammatory mesothelial surface. Twenty-five of 25 non-fluorescent areas were confirmed to benign; there were no false-negatives. These results conferred a sensitivity of 100%, a specificity of 52.1%, a positive-predictive value of 71.9%, and a negative predictive value of 100% and echoed results found during pleural biopsy (Table 2).

By macroscopic fluorescent assessment, the mean SBR of fluorescent MPM lesions was 3.1 (SD, 0.7) versus 2.8 (SD,0.6) in fluorescent lesions that were benign; p=0.03. Furthermore, MPM lesions displayed higher fluorescence levels than benign areas (both fluorescent and non-fluorescent); mean SBR of 3.1 (SD, 0.7) versus 2.1 (SD, 0.8); p<0.0001 (Figure 2j). Upon semi-quantitative microscopic NIR analysis of the 109 samples, ICG accumulation

was confirmed to be predominantly within areas correlating to histopathologically confirmed MPM (Figure 3).

FGS with ICG identifies occult residual disease that persists of “macroscopic resection” (Cohort 2)

For each of the 13 subjects enrolled in Cohort 2, the surgeon was able obtain what was felt to be complete macroscopic (R1) resection. Following R1 resection, the ipsilateral hemithorax of each subject was evaluated with NIR imaging to assess for residual disease. In 10 of 13 subjects, residual fluorescent foci were identified (representative examples provided in Figure 4). In total, 56 residual lesions were identified with a median number of 5.6 lesions/patient (range, 0 to 11). The mean size of these lesions was 0.3cm (range, 0.1 to 1.5cm). Residual lesions were frequently identified in (1) “difficult-to-reach” anatomic locations including the costophrenic sulcus and directly adjacent to thoracotomy site or (2) areas of significant pleural stripping, and where acute inflammation and blood shielded them from traditional visual identification. Surprisingly, we did identify deposits as large as 1.5cm within the operative field which were unidentifiable until highlighted by NIR imaging. All lesions were safely resected.

Upon final histopathologic review of the 56 residual foci identified by NIR imaging, 32 were found to be MPM deposits, 8 were benign lymph nodes, and 16 were inflamed pleura or adipose. Using final histopathologic evaluation, the PPV of NIR imaging was found to be 57.2%. Of note, the mean SBR of MPM confirmed biopsies was 3.2 versus 2.4 in benign biopsies (p=0.008). These values were similar to the SBR of MPM and benign lesions observed previous analyses (p=0.21 and p=0.17, respectively).

Feasibility and Practicality of FGS for MPM

Intraoperative imaging added a median of 7 minutes (range, 4 minutes to 13 minutes) to the case duration. Imaging was displayed in real-time on traditional OR monitors. Among the surgeons participating in this study, the technology was felt to provide additional useful information, found to be user-friendly and reliably improved the surgeons’ ability to identify residual disease. All four surgeons recommended continued investigation of this technology in the setting of MPM.

Comment

Although there remains no clear current standard-of-care treatment for MPM, trimodal therapy provides the best opportunity for prolonged survivorship for patients with limited disease (1, 2, 17, 18). Even with this aggressive approach, most patients suffer local disease recurrence (5, 6). In this exploratory study, we provide the first human evidence demonstrating that NIR imaging can provide real-time visual cues that allow for reproducible identification of residual disease during MPM cytoreduction. This information suggests that this approach may be a safe and practical tool that may improve cytoreduction and potentially local recurrence rates for MPM.

TumorGlow® is an approach that involves preoperative delivery of the near-infrared optical contrast agent, ICG. TumorGlow® utilizes ICG as a tumor mapping agent as described by

our group for central nervous system tumors (15), pulmonary metastases (10), and primary lung neoplasms (11). TumorGlow® requires delivery of ICG at a high dose (5mg/kg) with imaging occurring approximately 24 hours following drug delivery. Even at higher dosing levels of ICG, this approach was safe. Only one subject suffered a drug-related adverse event, which was transient catheter-site discomfort during drug infusion. Symptoms improved after decreasing the infusion rate and subsequently resolved, with no sequalae. No other adverse events were noted within this cohort. The low toxicity profile in MPM is in accordance with our experiences with central nervous system malignancies and other pulmonary malignancies (10, 11, 15).

In terms of practicality, TumorGlow® only required minor modifications to standard work flow. Subjects were infused as an outpatient 24 hours prior to surgery and discharged. The following morning, patients presented to the preoperative area per routine. During biopsy or resection, patients were imaged with standard thoracoscopic instruments equipped with NIR cameras/light sources, with real-time videos displayed on standard operating room monitors. Overall, imaging added 7 minutes to cases. Surgeons participating in the study found the technology helpful, minimally intrusive, and easy to use. Patients were generally enthusiastic and willing to participate despite the logistics requiring an additional visit for drug infusion.

During NIR imaging, fluorescent signal was present in 100% of MPM lesions sampled and identifiable in deposits as small as 1mm. These results were also reproducible following neoadjuvant chemotherapy. Reproducible fluorescence is likely related to the superficial nature of MPM, which is favorable for NIR imaging and other optical imaging approaches. Similar results have also been noted during NIR imaging for intraabdominal debulking of peritoneal carcinomatosis (19). Although noting excellent sensitivity, the observed false-positive rate was 30%. Given the chronic inflammatory nature of mesothelioma, it is not surprising that background ICG accumulation was typically found in hyperemic, non-cancerous tissues marked by leaky capillaries. These vascular abnormalities result in off-target dye extravasation through the EPR effect. Despite inaccuracies, we believe a highly sensitive tool is more appropriate than one that errs on the side of specificity, particularly within the context of cytoreductive surgery.

It is important to interpret these findings within the context of our study design. Our inclusion criteria required subjects be deemed surgical candidates prior to enrollment, which may artificially inflate some of the test characteristics of TumorGlow® by increasing pre-test probabilities. We accept this limitation as we envision this technology serving as an adjunct to, not a replacement for, current diagnostics and therapeutics (20). Secondly, determining an actual false-negative rate is challenging. Determination of “false negatives” would require the true denominator (likely only feasible with a rapid autopsy study). This is an important consideration as microscopic disease is likely below the current thresholds of NIR detection. Despite these limitations, the provided data clearly suggests that TumorGlow® allows for detection of more MPM lesions than intraoperative inspection alone.

Notwithstanding limitations, this report marks the first successful attempt of optical surgical navigation for MPM. NIR feedback provides the thoracic surgeon with a unique tool that can improve detection of residual disease following MPM surgery by providing real-time visual information. TumorGlow® may provide an opportunity to improve upon the poor prognosis associated with MPM, and ultimately improve upon high current local recurrence rates. Further work aimed at optimizing this approach is underway for MPM and a variety of other pleural- and chest wall-based neoplasms.

References

1. Wolf AS, Flores RM. Current treatment of mesothelioma: Extrapleural pneumonectomy versus pleurectomy/decortication. Thorac Surg Clin. 2016; 26(3):359–375. [PubMed: 27427530]
2. Chan WH, Sugarbaker DJ, Burt BM. Intraoperative adjuncts for malignant pleural mesothelioma. Transl Lung Cancer Res. 2017; 6(3):285–294. [PubMed: 28713674]
3. Vogelzang NJ, Rusthoven JJ, Symanowski J, et al. Phase iii study of pemetrexed in combination with cisplatin versus cisplatin alone in patients with malignant pleural mesothelioma. J Clin Oncol. 2003; 21(14):2636–2644. [PubMed: 12860938]
4. Krug LM, Pass HI, Rusch VW, et al. Multicenter phase ii trial of neoadjuvant pemetrexed plus cisplatin followed by extrapleural pneumonectomy and radiation for malignant pleural mesothelioma. J Clin Oncol. 2009; 27(18):3007–3013. [PubMed: 19364962]
5. Baldini EH, Richards WG, Gill RR, et al. Updated patterns of failure after multimodality therapy for malignant pleural mesothelioma. J Thorac Cardiovasc Surg. 2015; 149(5):1374–1381. [PubMed: 25772281]
6. Flores RM, Pass HI, Seshan VE, et al. Extrapleural pneumonectomy versus pleurectomy/decortication in the surgical management of malignant pleural mesothelioma: Results in 663 patients. J Thorac Cardiovasc Surg. 2008; 135(3):620–626. 626e621–623. [PubMed: 18329481]
7. de Perrot M, Feld R, Leighl NB, et al. Accelerated hemithoracic radiation followed by extrapleural pneumonectomy for malignant pleural mesothelioma. J Thorac Cardiovasc Surg. 2016; 151(2):468–473. [PubMed: 26614413]
8. Rusch VW, Figlin R, Godwin D, Piantadosi S. Intrapleural cisplatin and cytarabine in the management of malignant pleural effusions: A lung cancer study group trial. J Clin Oncol. 1991; 9(2):313–319. [PubMed: 1988578]
9. Ris HB. Photodynamic therapy as an adjunct to surgery for malignant pleural mesothelioma. Lung Cancer. 2005; 49(Suppl 1):S65–68. [PubMed: 15916831]
10. Keating J, Newton A, Venegas O, et al. Near-infrared intraoperative molecular imaging can locate metastases to the lung. Ann Thorac Surg. 2016
11. Okusanya OT, Holt D, Heitjan D, et al. Intraoperative near-infrared imaging can identify pulmonary nodules. Ann Thorac Surg. 2014; 98(4):1223–1230. [PubMed: 25106680]
12. Jiang JX, Keating JJ, Jesus EM, et al. Optimization of the enhanced permeability and retention effect for near-infrared imaging of solid tumors with indocyanine green. Am J Nucl Med Mol Imaging. 2015; 5(4):390–400. [PubMed: 26269776]
13. Predina, JNA; Keating, J; Dunbar, A; Connolly, C; Singhal, S. Near-infrared intraoperative molecular imaging can enhance malignant pleural mesothelioma resection. The 25th Annual Meeting of the Asian Society for Cardiovascular and Thoracic Surgery; Seoul, Korea. 2017;
14. Keating J, Newton A, Venegas O, et al. Near-infrared intraoperative molecular imaging can locate metastases to the lung. Ann Thorac Surg. 2017; 103(2):390–398. [PubMed: 27793401]
15. Lee JY, Thawani JP, Pierce J, et al. Intraoperative near-infrared optical imaging can localize gadolinium-enhancing gliomas during surgery. Neurosurgery. 2016; 79(6):856–871. [PubMed: 27741220]
16. SERVICES USDOHAH. Common terminology criteria for adverse events (ctcae) version 4.0. 2010.

17. Network NCC. NCCN Guidelines. 2017. Nccn clincal practice guidelins in oncology: Malignant plerual mesothelioma.

18. van Meerbeeck JP, Scherpereel A, Surmont VF, Baas P. Malignant pleural mesothelioma: The standard of care and challenges for future management. Crit Rev Oncol Hematol. 2011; 78(2):92–111. [PubMed: 20466560]

19. Hoogstins CE, Tummers QR, Gaarenstroom KN, et al. A novel tumor-specific agent for intraoperative near-infrared fluorescence imaging: A translational study in healthy volunteers and patients with ovarian cancer. Clin Cancer Res. 2016; 22(12):2929–2938. [PubMed: 27306792]

20. Predina JD, Newton AD, Keating J, et al. Intraoperative molecular imaging combined with positron emission tomography improves surgical management of peripheral malignant pulmonary nodules. Ann Surg. 2017

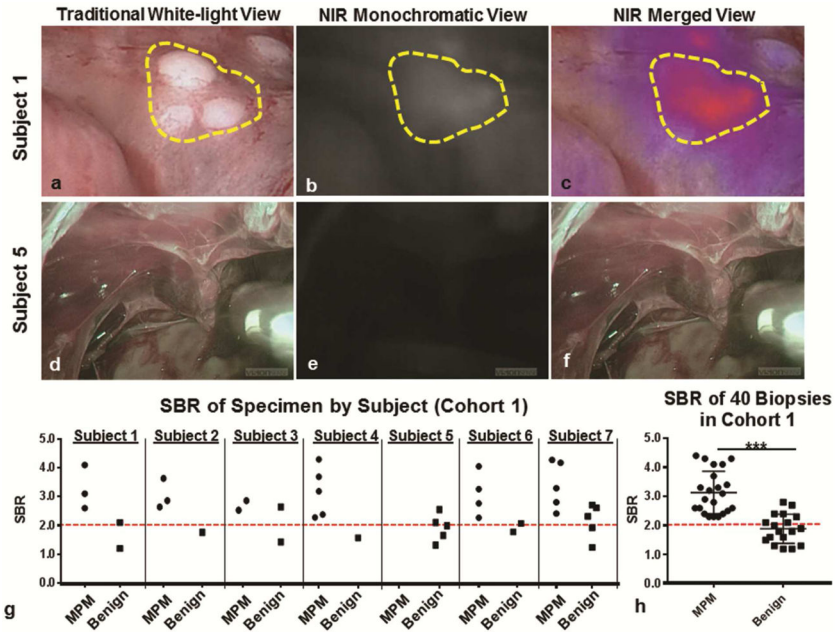

Figure 1.

FGS with ICG identified MPM during pleural biopsy: Subject 1: Representative example of subject in which high levels of fluorescence were observed during pleural biopsy. Subject 1, sample images of a cluster of 1mm MPM lesions (yellow gate) are displayed in a (a) traditional white-light view, (b) a monochromatic NIR view and (c) a merged NIR view. In Subject 5, there were no lesions identified during (d) white light thoracoscopy, nor during (d) NIR monochromatic or (e) merged NIR evaluation. (g) For each subject, the SBR of biopsied lesions were recorded and categorized based on final pathologic diagnosis. (h) The fluorescence (SBR) of biopsy proven MPM was significantly higher than benign lesions ($p<0.0001$).

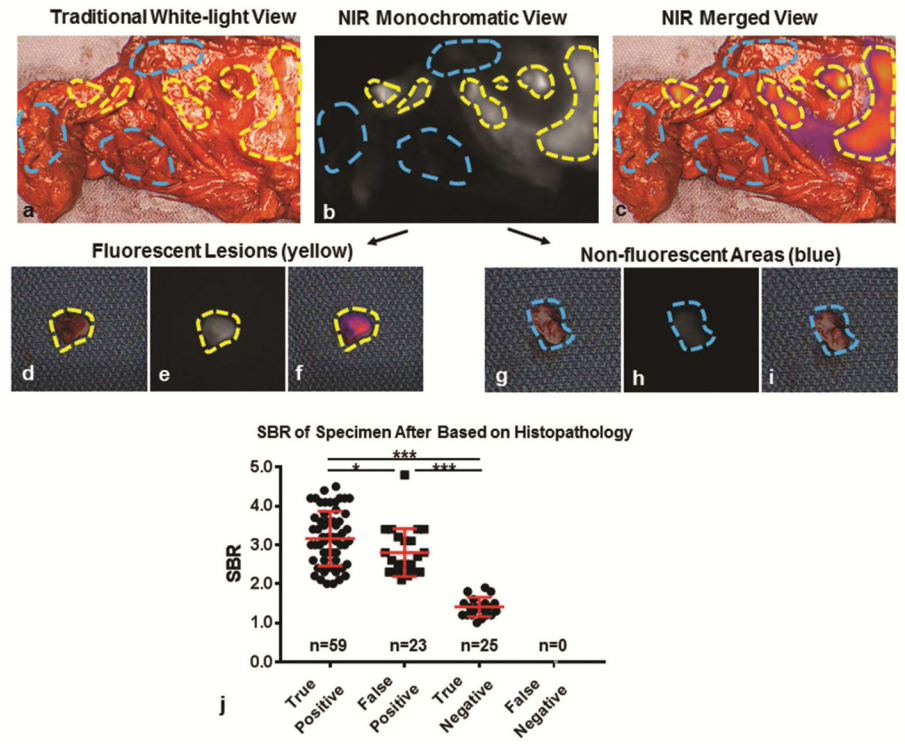

Figure 2.

ICG accumulates in resected MPM and displays fluorescence during cytoreductive surgery: Subject 12: Representative example of post-resection macroscopic and microscopic semi-quantitative fluorescence evaluation. Resected specimen were evaluated *ex vivo* using a combination of white-light views (**a**) and NIR views (**b–c**). Using NIR fluorescence patterns, fluorescent samples (*yellow gate*) and non-fluorescent samples (*blue gate*) were isolated, and submitted individually by a pathologist. As can be seen, fluorescent lesions were cleanly dissected from surrounding tissue (**d–f**), while non-fluorescent areas were also obtained (**g–i**). After obtaining a pathologic diagnosis for each submitted specimen (n=107), we plotted SBR for true-positives, false-positives, true-negatives and false-negatives. We found that the SBR of fluorescent MPM lesions (true positives) was higher than benign lesions which displayed fluorescence (false positives); p=0.03 (**j**). Both true positives and false positives displayed significantly higher fluorescence patterns than non-fluorescent benign tissues (true negatives); p<0.001. * - p<0.05; *** - p<0.0001

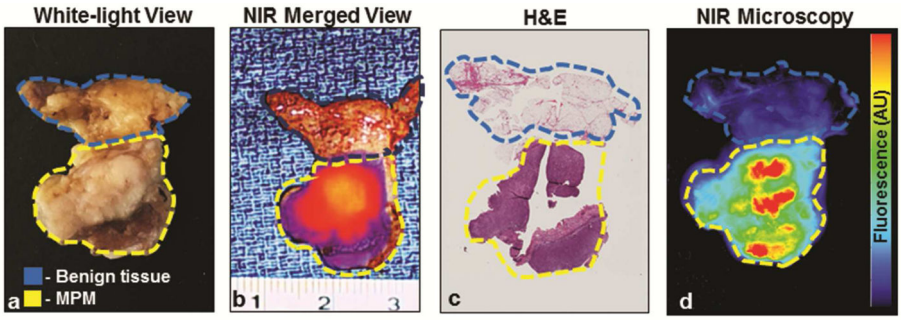

Figure 3.

NIR Imaging with ICG accumulates preferentially in MPM. Specimens resected by standard-of-care approaches underwent macroscopic fluorescent profiling using a combination of standard white-light views (**a**), NIR views and NIR merged views (**b**). All resected specimens then underwent a series of histopathologic (**c**) and microscopic fluorescent analyses (**d**) to determine accuracy and patterns of dye accumulation. yellow gate—tumor by histopathologic review; blue gate—benign tissue by histopathologic analysis.

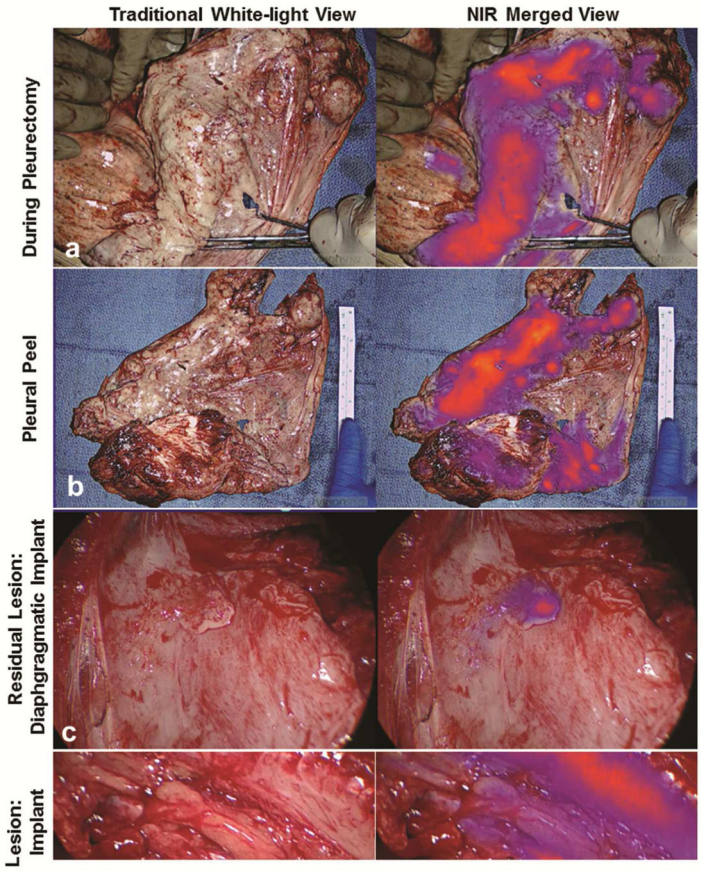

Figure 4.

FGS with ICG identifies occult macroscopic residual disease following complete resection. Following macroscopic resection using white-light only, the ipsilateral hemithorax was then evaluated in NIR imaging to determine if residual disease was present. Data from Subject 10 is used to illustrate the workflow. The surgeon first completed P/D (**a**). All resected specimens underwent *ex vivo* macroscopic fluorescence evaluation **(b)**. Next, the chest was reevaluated with NIR imaging to assess for residual disease. An example of a diaphragmatic implant (**c**) and an intercostal lesion (**d**) are provided. Both lesions were MPM by histopathologic review.

Table 1

Subject Characteristics and Safety Data.

Subject ID	Age (years)	Gender	Laterality	Disease Histology	Pt Weight (kg)	ICG infused (mg)	Time to imaging (h)
Cohort 1							
1	66	Male	Right	MPM-epitheliod	80.5	402.5	28.5
2	67	Male	Left	MPM-epitheliod	87.6	438	27.6
3	71	Male	Right	MPM-mixed	56.7	283.5	28.2
4	57	Female	Right	MPM-epitheliod	41.8	209	22.5
5	80	Male	Right	Benign Inflammation	81.7	408.5	30.4
6	82	Male	Left	MPM-sarcomatoid	61.2	306	23.0
7	75	Female	Right	MPM-sarcomatoid	86.2	204 *	26.3
Cohort 2							
8	71	Female	Right	MPM-epitheliod	88.2	441	27.0
9	69	Female	Left	MPM-epitheliod	61.2	306	23.0
10	59	Male	Right	MPM-epitheliod	116.1	580.5	22.3
11	64	Male	Left	MPM-epitheliod	62.3	311.5	19.3
12	58	Male	Left	MPM-epitheliod	64.1	320.5	22.3
13	68	Male	Right	MPM-epitheliod	72.6	363	24.2
14	54	Male	Right	MPM-epitheliod	81.2	406	26.4
15	62	Female	Left	MPM-epitheliod	65.2	326	18.6
16	71	Male	Right	MPM-epitheliod	78.0	390	22.3
17	65	Male	Left	MPM-epitheliod	82.3	411.5	23.1
18	74	Male	Left	MPM-epitheliod	74.5	372.5	26.4
19	79	Female	Left	MPM-epitheliod	72.1	360.5	25.3
20	63	Male	Right	MPM-epitheliod	81.6	408	23.7

* infusion stopped after adverse event

Ann Thorac Surg. Author manuscript; available in PMC 2020 January 01.

Table 2

Contingency table displaying test characteristics of intraoperative NIR imaging for pleural biopsies (from Cohort 1)

	MPM*	Benign Lesion*
NIR Imaging		
Fluorescent (SBR≥ 2)	22	7
Non-fluorescent (SBR<2)	0	11
	Sensitivity *–100%* (95% CI: 81.5% – 100%) ***Specificity*** – 61.1% (95% CI: 36.1% – 81.7%) ***PPV*** – 75.80% (95% CI: 55.8% – 84.8%) ***NPV*** – *100%* (95% CI: 67.8% – 100%)	

*Gold Standard Diagnosis by final pathologic review. NIR-near infrared; SBR-signal to background fluorescent ratio, PPV-positive predictive value, NPV-negative predictive value, 95% CI-95% confidence interval

Table 3

Contingency table displaying test characteristics of *ex vivo* NIR imaging of resected specimen (from Cohort 2)

	MPM*	Benign Lesion*
NIR Imaging		
Fluorescent (SBR≥ 2)	59	23
Non-fluorescent (SBR<2)	0	25
	Sensitivity *–100%* (95% CI: 93.9% – 100%) ***Specificity*** – 52.1% (95% CI: 37.1% – 66.7%) ***PPV*** – 71.9% (95% CI: 65.4% – 77.5%) ***NPV*** – *100%* (95% CI: 83.4% – 100%)	

*Gold Standard Diagnosis by final pathologic review. NIR-near infrared; SBR-signal to background fluorescent ratio, PPV-positive predictive value, NPV-negative predictive value, 95% CI-95% confidence interval